

# Regiospecific Control of Protein Expression in Cells Cultured on Two-Component Counter Gradients of Extracellular Matrix Proteins

Rico C. Gunawan,<sup>†</sup> Eric R. Choban,<sup>†</sup> John E. Conour,<sup>‡</sup> Jonathan Silvestre,<sup>†</sup> Lawrence B. Schook,<sup>‡,§</sup> H. Rex Gaskins,<sup>‡,§</sup> Deborah E. Leckband,<sup>\*,†,§</sup> and Paul J. A. Kenis<sup>\*,†,§</sup>

Department of Chemical and Biomolecular Engineering, Department of Animal Sciences, and Institute for Genomic Biology, University of Illinois at Urbana–Champaign, 600 South Matthews Avenue, Urbana, Illinois 61801

Received July 7, 2004. In Final Form: December 14, 2004

This work describes the use of microfluidic tools to generate covalently immobilized counter gradients of extracellular matrix (ECM) proteins laminin and collagen I. Using these platforms, we demonstrate control of the expression levels of two proteins linked to cell cycle progression by virtue of the spatial location of cells on the gradients, and hence by the local ECM environments in these devices. In contrast to physisorbed gradients, covalently immobilized protein patterns preserved the gradient fidelity, making long term cell studies feasible. This method of precisely controlling local cell environments is simple and broadly portable to other cell types and to other ECM proteins or soluble factors. Our approach promises to enable new investigations in cell biology that will contribute to the establishment of biological design rules for controlling cell growth, differentiation, and function.

## Introduction

The identification and study of the constellation of factors that control cell behavior is key to many cell biology studies. Both the quantification of components in the tissue microenvironment and their quantitative control are formidable obstacles to determining the biological design rules that control cell behavior in vivo. There is an urgent need for in vitro models that enable investigations of cell behavior in complex but precisely controlled microenvironments. Although the ever-increasing ability to fabricate and pattern structures at the microscale has long promised to provide such models or platforms, those reported to date have been few in number and of limited utility. In addition, in many systems, the effect of only a few factors can be studied simultaneously. Furthermore, the instability of some engineered microenvironments limits investigations to less than 24 h. This paper describes novel in vitro platform technology that is broadly applicable to the study of a wide range of cellular events including proliferation, differentiation, chemotaxis, polarity development, and cell migration, as a function of precisely controlled, multicomponent microenvironments that persist for days.

Cells are postulated to respond to extracellular matrix (ECM) concentration gradients in vivo during, for example, organogenesis and in the immune response.<sup>1,2</sup> Numerous examples exist in vivo, in which either soluble or immobilized gradients are thought to control cell function and differentiation. In the specific example of the small

intestinal mucosa, two morphologically and functionally distinct compartments characterize the self-renewing epithelium: namely, the crypts of Lieberkühn and epithelial villi (Figure 1A). This biological system represents one of the many biological examples in which the microenvironment is believed to direct the commitment of stem cells to one of four primary cell types: enterocytes, enteroendocrine cells, goblet cells, and Paneth cells. The commitment of stem cells toward these cell lineages is regulated by growth factors,<sup>3</sup> luminal nutrients,<sup>4</sup> and ECM components, which are differentially encountered along the crypt–villus axis.<sup>5,6</sup> Importantly, the regiospecific expression profiles of laminin isoforms along the crypt–villus axis (Figure 1A) correspond to the transition of epithelial cells from the proliferative crypt zone to the villus, where they undergo terminal differentiation.<sup>7</sup> Specific laminin–integrin interactions influence cell cycle progression through various intracellular signaling pathways.<sup>8</sup> In addition, integrins expressed on intestinal epithelial cells exhibit regiospecific distribution patterns along the crypt–villus axis, thus adding an additional level of complexity to investigations of ECM–epithelial cell interactions in vivo.<sup>7</sup> Although laminin isoforms induce differentiation in some epithelial cell lines,<sup>9</sup> a major question remains: to what extent does the ECM microenvironment control stem cell differentiation? The lack of in vitro models that adequately simulate the in vivo ECM environment has been a chief obstacle to addressing this issue.

\* Corresponding author. Deborah E. Leckband: telephone, 217-244-0793; fax, 217-333-5052; e-mail, leckband@scs.uiuc.edu. Paul J. A. Kenis: telephone, 217-265-0523; fax, 217-333-5052; e-mail, kenis@uiuc.edu.

<sup>†</sup> Department of Chemical and Biomolecular Engineering.

<sup>‡</sup> Department of Animal Sciences.

<sup>§</sup> Institute for Genomic Biology.

(1) Carmeliet, P. *Nat. Med.* **2000**, *6*, 389–395.

(2) Neumann, C.; Cohen, S. *Bioessays* **1997**, *19*, 721–729.

(3) Hardin, J. A.; Buret, A.; Meddings, J. B.; Gall, D. G. *Am. J. Physiol.* **1993**, *264*, G221–226.

(4) Turowski, G.; Rashid, Z.; Hong, F.; Madri, J. A.; Basson, M. D. *Cancer Res.* **1994**, *54*, 5974–5980.

(5) Ingber, D. E.; Madri, J. A.; Jamieson, J. D. *Am. J. Pathol.* **1986**, *122*, 129–139.

(6) Madri, J. A.; Basson, M. D. *Lab. Invest.* **1992**, *66*, 519–521.

(7) Beaulieu, J.-F. *Front. Biosci.* **1999**, *4*, d310–321.

(8) Giancotti, F. G. *Curr. Opin. Cell Biol.* **1997**, *9*, 691–700.

(9) Simon-Assmann, P.; Lefebvre, O.; Bellissent-Waydelich, A.; Olsen, J.; Orian-Rousseau, V.; De Arcangelis, A. *Ann. N.Y. Acad. Sci.* **1998**, *859*, 46–64.

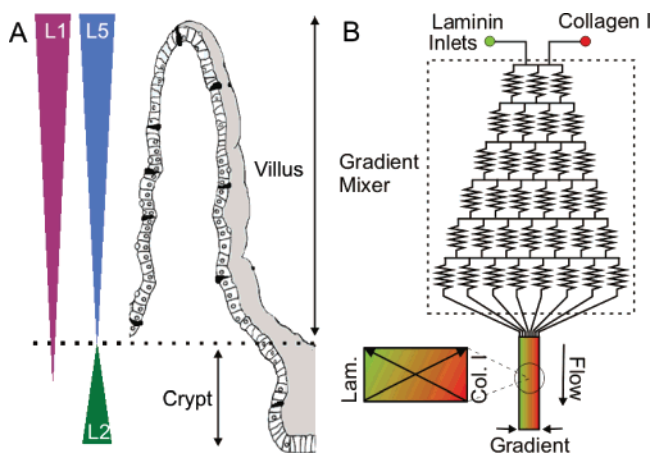


**Figure 1.** Patterns of ECM proteins of crypt-villus epithelium mimicked using microfluidic platforms. (A) Expression of laminin isoforms laminin 1 (L1), laminin 5 (L5), and laminin 2 (L2) along the crypt-villus axis of small intestine (ref 7). (B) Microfluidic gradient maker used to recreate ECM protein gradients (ref 15). Pure laminin and collagen I solutions were injected at the inlets. As they flow through the channels, they split and mix in the microfluidic gradient maker. Finally, all streams containing different concentrations convene in the main channel to form gradients perpendicular to the direction of flow.

By harnessing the distinct properties of fluid flow at the microscale, most notably laminar flow, microfluidic platforms enable the study of cells in precisely defined microenvironments, including both immobilized and diffusional gradients.<sup>10</sup> The lack of turbulent mixing at the microscale generates laminar flow of parallel fluid streams of different composition that mix only by slow interdiffusion. This in turn generates *stepwise solution gradients* that can be used to pattern surfaces with different proteins and different cells, while enabling the spatial control of the medium surrounding individual cells, to selectively expose cells or parts of cells to soluble triggers.<sup>11,12</sup> Recently, Jeon et al. demonstrated the use of smooth gradients of interleukin-8 in solution, to study the impact of soluble gradients on chemotaxis.<sup>13</sup> However, the fact that solution gradients require continuous flow limits their utility in cell studies. This is because they can only be performed for a few hours due to the large consumption of reagents and to the flow-induced shear stresses that may affect cell responses. Moreover, haptotactic cell responses *in vivo* are determined by static, immobilized gradients.<sup>14</sup>

To generate immobilized gradients, Dertinger et al. developed methodology to transfer solution gradients onto a surface by physisorption.<sup>15</sup> They thus investigated directional neurite outgrowth on laminin gradients.<sup>15,16</sup> Immobilization via physisorption, however, does not ensure the preservation of the local surface composition for more than a day. Factors including surface diffusion, protein desorption, and cell-induced degradation remodel

the gradients over time, thereby limiting the use of physisorbed gradients to short-term cell studies.

This paper describes the fabrication and validation of broadly applicable platforms comprised of surface-immobilized gradients for controlling and studying cell function. This development overcomes the limitations of both solution and physisorbed surface gradients and enables the study of cell behavior as a result of complicated, stable multispecies gradients of a wide variety of ECM components over several days. The positional control of cell responses on spatial, covalently immobilized counter gradients of the ECM proteins laminin and collagen I is demonstrated. Cell responses to the engineered microenvironments were quantified with expression markers of cell cycle progression. We investigated three different cell types cultured on these gradients: namely, in rat IEC-6 intestinal crypt-like cells, in human colonic adenocarcinoma (Caco-2<sub>BBE</sub>) cells, and in Chinese hamster ovary (CHO) fibroblasts. The findings validate the spatial control of differences in the expression of protein markers for cell cycle progression that were linked directly to the local laminin/collagen I concentration ratio defined by the spatial position of the cells on the gradient. These results illustrate the broad potential utility of these novel platforms for further investigations of cell behavior, including differentiation, migration,<sup>16</sup> and proliferation that are governed by the cell microenvironment.

## Materials and Methods

**Substrate Preparation.** The substrates consisted of self-assembled, carboxy-terminated alkanethiol monolayers on gold films. Glass slides (Fisher Scientific, Pittsburgh, PA) were cleaned by boiling in a piranha solution (HCl:H<sub>2</sub>O<sub>2</sub>:H<sub>2</sub>O = 1:1:1) for 20 min. They were subsequently rinsed with water and ethanol and dried with nitrogen. Gold (A-1-Coin Buyers, Champaign, IL) was thermally deposited onto the glass slides in a thermal evaporator (Cooke Vacuum Products, Inc., Norwalk, CT) at a base pressure of 10<sup>-6</sup> Torr. An adhesion promoter, chromium (R.D. Mathis Co., Long Beach, CA), with a thickness of 10 Å was first deposited onto the glass slides at a rate of 0.1 Å/s. The gold films were then deposited at 1 Å/s with a final thickness of 500 Å. After deposition, the gold substrates were immersed overnight in a solution of 1 mM 16-mercaptohexadecanoic acid and 11-mercaptoundecan-1-ol (Sigma, St. Louis, MO) at a 3:1 molar ratio (1 mM total alkanethiol). The substrates were then rinsed with ethanol and dried with filtered nitrogen.<sup>17</sup>

**Uniformly-Coated Protein Substrates.** Patterns of proteins with uniform mass coverage were generated inside a microfluidic network that was molded in poly(dimethylsiloxane) (PDMS) (Dow Corning, Midland, MI). A PDMS microfluidic network (Figure 1B) was placed onto a gold substrate coated with a self-assembled monolayer (SAM). The gold substrate and the PDMS slab were then sandwiched between two Plexiglass slabs. The alkanethiol monolayer confined in the 100-micron channels was activated with a mixture of 1-ethyl-3-(3-dimethylaminopropyl) carbodiimide HCl (EDC) and *N*-hydroxysuccinimide (NHS), both from Pierce (Rockford, IL).<sup>18</sup> A 0.5 mL solution of EDC/NHS (3.8 mg EDC/mL and 6.7 mg NHS/mL in 0.5 M acetate buffer, pH 5.5) was then passed through the channels for 15 min at a flow rate of 0.03 mL/min. This was followed by rinsing with 0.2 mL of acetate buffer to remove unreacted EDC/NHS. The channels were then filled with the protein solution, incubated for 2 h at room temperature, and then rinsed with 0.2 mL of acetate buffer. The protein solutions consisted of a mixture of laminin and collagen I, a mixture of laminin and bovine serum albumin (BSA), and a mixture of collagen I and BSA. Laminin and collagen I were mixed at laminin molar percentages of 0%, 20%, 40%, 60%, 80%, and 100% (0.1 mg/mL total protein). Laminin/BSA were mixed at molar percentages of 25%, 50%, and 75% laminin, and collagen

(10) Colton, I. J.; Carbeck, J. D.; Rao, J.; Whitesides, G. M. *Electrophoresis* **1998**, *19*, 367–382.

(11) Takayama, S.; McDonald, J. C.; Ostuni, E.; Liang, M. N.; Kenis, P. J.; Ismagilov, R. F.; Whitesides, G. M. *Proc. Nat. Acad. Sci. U.S.A.* **1999**, *96*, 5545–5548.

(12) Takayama, S.; Ostuni, E.; LeDuc, P.; Naruse, K.; Ingber, D. E.; Whitesides, G. M. *Nature* **2001**, *411*, 1016.

(13) Jeon, N. L.; Baskaran, H.; Dertinger, S. K. W.; Whitesides, G. M.; Van De Water, L.; Toner, M. *Nat. Biotechnol.* **2002**, *20*, 826–830.

(14) Brandley, B. K.; Schnaar, R. L. *Dev. Biol.* **1989**, *135*, 74–86.

(15) Dertinger, S. K. W.; Chiu, D. T.; Jeon, N. L.; Whitesides, G. M. *Anal. Chem.* **2001**, *73*, 1240–1246.

(16) Dertinger, S. K. W.; Jiang, X.; Li, Z.; Murthy, V. N.; Whitesides, G. M. *Proc. Nat. Acad. Sci. U.S.A.* **2002**, *99*, 12542–12547.

(17) Laibinis, P. E.; Whitesides, G. M.; Allara, D. L.; Tao, Y.-T.; Parikh, A. N.; Nuzzo, R. *J. Am. Chem. Soc.* **1991**, *113*, 7152–7167.

(18) Fung, Y. S.; Wong, Y. Y. *Anal. Chem.* **2001**, *73*, 5302–5309.



I/BSA were mixed at 25%, 50%, 75%, and 100% collagen. After rinsing the channels with buffer, the Plexiglass and PDMS slabs were peeled off, and the substrates were blocked with 0.3 mL of a 10% (w/w) solution of BSA in PBS for 15 min at room temperature. The substrates were rinsed with PBS and sterile water and then dried in air.

**Surface ECM Gradient Preparation.** The microfluidic gradient tool (Figure 1B), which was used to generate patterns of protein gradients, comprises a network of microchannels in PDMS with the modified gold substrate as the base. The microchannels were fabricated using rapid prototyping and soft lithography.<sup>19</sup> Inlet and outlets were created using a steel punch. Polyethylene tubing inserted into these ports served to deliver fluid to the microchannels. The gold substrate and the PDMS microchannels were brought into contact and "sandwiched" between two Plexiglass slabs. To prevent leakage during fluid injection, the assembly was clamped together with binder clips. Bubbles were purged from the microchannels by first injecting ethanol and then rinsing the channels with distilled water followed by acetate buffer (0.5 M sodium acetate, pH 5.5). A 0.5 mL volume of EDC/NHS solution was then injected through the microchannel. After 15 min at room temperature, the channels were rinsed with 0.3 mL of acetate buffer to remove unreacted EDC/NHS. Approximately 0.2 mL each of laminin and collagen I (BD Biosciences, Bedford, MA) in 0.5 M acetate buffer at pH 5.5 were then pumped through the microchannels at a flow rate between 0.3 and 0.9  $\mu\text{L}/\text{min}$  at 4 °C using a syringe pump (PHD 2000, Harvard Apparatus, Holliston, MA). The unreacted groups on the substrate were then blocked to prevent nonspecific adsorption with 0.2 mL of 10% bovine serum albumin (Sigma) in PBS (10 mM phosphate, 0.14 M NaCl, pH 7.4). The PDMS mold was then removed from the substrate, and the exposed gold surface was blocked with 10% BSA in PBS for 15 min at 4 °C. Physically adsorbed gradients were prepared similarly without using the EDC/NHS coupling agents.

**Surface ECM Gradient Characterization.** Immobilized gradients of laminin and collagen I were stained with, respectively, anti-laminin (rabbit, 1:50 in 10% BSA/PBS, Sigma) and anti-collagen I (mouse, 1:100 in 10% BSA/PBS, Sigma) for 10 min at room temperature. After rinsing with PBS, secondary antibodies, anti-rabbit IgG labeled with FITC (1:200 in 10% BSA/PBS, Sigma), and anti-mouse IgG labeled with Alexa Fluor 568 (1:100 in 10% BSA/PBS, Molecular Probes, Portland, OR) were applied for 10 min. The substrate was then rinsed with PBS, treated with an Antifade kit (Molecular Probes) to maintain the fluorescence intensity, and then covered with a coverslip. Fluorescent images were visualized with a Nikon Optiphot-2 microscope (Fryer, Carpentersville, IL) equipped for epifluorescence. Digital images were captured with Image-Pro Plus software, version 3.3 (Media Cybernetics, Silver Spring, MD). To quantify intensity changes across the gradients, 15 intensity profiles across the laminin and collagen I gradients were measured and averaged for each gradient to give the mean fluorescence intensity (MFI) profile. The fluorescence intensity was then calibrated in terms of the protein surface density, using surface plasmon resonance.

**Calibration of Protein Surface Densities by Surface Plasmon Resonance (SPR).** The covalent attachment of laminin to monolayers was quantified using a home-built SPR.<sup>20</sup> The SPR cell (0.25 mL volume), containing a uniform self-assembled alkanethiol monolayer, was rinsed consecutively with water and acetate buffer (0.5 M sodium acetate/acetic acid, pH 5.5) for 15 min. This was followed by activation with EDC/NHS for 15 min at a flow rate of 4 mL/h. The unreacted reagents were flushed from the cell by flowing acetate buffer through the channel for 5 min. Laminin or collagen I was injected through the cell at a rate of 0.5 mL/h. Finally, the SPR cell was rinsed with acetate buffer, followed by water for 10 min at a flow rate of 4 mL/min. The optical thickness  $\Delta d$  of the bound protein was calculated by fitting Fresnel dispersion equations to the change in the plasmon resonance angle  $\Theta_r$ . A calibration slope  $k$  was determined using the refractive index  $n$  of the sample material in the dry state.

With this slope, the changes in the resonance angle  $\Theta_r$  can be directly related to the optical thickness,  $\Delta d$  of the adsorbed material. The changes in the effective optical thickness,  $\Delta d_r$ , are readily converted into protein surface coverage by the following equation:

$$\Gamma = \rho \Delta d \quad (1)$$

In this study, we used a refractive index of 1.46 for both the laminin and collagen I.<sup>21</sup>

The protein surface density on the patterns was determined by correlating the surface density quantified by SPR with the MFI of uniform protein films prepared under identical conditions. We first quantified the surface densities of covalently bound laminin and collagen I films prepared with protein solution concentrations of 0.025, 0.01, and 0.005 mg/mL, and then quantified the corresponding fluorescence intensities of stained laminin and collagen I films prepared under identical conditions. The calibration curve, obtained by relating the absolute protein density to the MFI, was then used to quantify the densities of laminin and collagen I on both the uniform protein stripes and the ECM gradients.

**Cell Culture.** The IEC-6 rat small intestine epithelial cells were cultured in Dulbecco's modified eagle medium (DMEM) supplemented with a final glucose concentration of 25 mM, 10% fetal bovine serum (FBS, Gemini Bio-Products, Woodland, CA), penicillin (10 000 U/mL), streptomycin (10 000  $\mu\text{g}/\text{mL}$ , BioWhittaker, Walkersville, MD), fungizone (250  $\mu\text{g}/\text{mL}$ , BioWhittaker), and 0.1  $\mu\text{g}/\text{mL}$  bovine insulin (Invitrogen, Carlsbad, CA). Caco-2<sub>BEE</sub> human colonic adenocarcinoma cells were cultured in DMEM supplemented with 10% FBS, 10 mg/mL transferrin, 2 mM glutamine, 1 mM pyruvate, 10 mM HEPES, 100 U/mL penicillin, and 0.1 mg/mL streptomycin. CHO cells were cultured in DMEM supplemented with 10% FBS, 1% penicillin/streptomycin, and 0.1% fungizone. Cells were maintained at 37 °C in a humidified incubator with 5% CO<sub>2</sub>. Cell monolayers (~90% confluence) were dissociated by incubation with trypsin-versene (BioWhittaker) for 5 min at 37 °C. Cells were resuspended in 10 mL of supplemented DMEM and centrifuged for 7 min at 1800 rpm. Cell pellets were resuspended in serum-free medium consisting of supplemented DMEM without FBS.

**Analysis of Protein Expression.** Cell cycle progression and exit were monitored by measuring the expression of proliferating cell nuclear antigen (PCNA)<sup>22</sup> and a cyclin-dependent kinase inhibitor (p27),<sup>23</sup> respectively, via immunofluorescence. The expression of the cell markers PCNA and p27 was determined by immunofluorescence 1 day and 3 days after the cells were cultured on uniform protein stripes and on the gradients. During the cell cycle, PCNA is expressed during the S-phase, which indicates that cells progress through the cell cycle. In contrast, p27 is expressed during the G<sub>1</sub>-phase, if cells exit the cell cycle and undergo a G<sub>0</sub> growth arrest. These two expression markers thus indicate differences in cell cycle progression in response to the local environment. Cells were fixed with 3.7% formaldehyde (Fisher, Fair Lawn, NJ) for 30 min and then blocked with 4% FBS in PBS for 15 min at 4 °C. Cells were then incubated with primary anti-PCNA antibody (PC-10, [1:40], Santa Cruz Biotechnology, Santa Cruz, CA), anti-p27 primary antibody (C-19, [1:50], Santa Cruz Biotechnology), and DAPI (1:200 of 150  $\mu\text{g}/\text{mL}$  stock solution, Sigma) for 30 min. Cells were then rinsed with PBS and stained with a goat anti-mouse IgG conjugated with Alexa Fluor (1:200, Molecular Probes) and a goat, anti-rabbit IgG conjugated with FITC (1:200, Sigma) for 30 min. They were finally treated with an Antifade kit (Molecular Probes). Fluorescent images were captured with a Nikon Optiphot-2 microscope and analyzed with Image-Pro Plus software.

For each uniform stripe, three parallel protein stripes were prepared and seeded with cells at a density of 10<sup>3</sup> cells/mm<sup>2</sup>. The

(21) Guemouri, L.; Ogier, J.; Ramsden, J. J. *J. Chem. Phys.* **1998**, *109*, 3265–3268.

(22) Kuldorff, M.; McShane, L. M.; Schatzkin, A.; Freedman, L. S.; Wargovich, M. J.; Woods, C.; Purewal, M.; Burt, R. W.; Lawson, M.; Mateski, D. J.; Lanza, E.; Corle, D. K.; O'Brien, B.; Moler, J. *J. Clin. Epidemiol.* **2000**, *53*, 875–883.

(23) Tian, J. Q.; Quaroni, A. *Am. J. Physiol. Cell Physiol.* **1999**, *276*, C1245–C1258.

(19) Xia, Y.; Rogers, J. A.; Paul, K. E.; Whitesides, G. M. *Chem. Rev.* **1999**, *99*, 1823–1848.

(20) Lavrik, N.; Leckband, D. *Langmuir* **2000**, *16*, 1842–1851.

fluorescence intensities were measured from 10–20 cells. For the gradient substrates, the fluorescence intensities were then measured from 80–100 cells. The fluorescence intensity was analyzed with ImageJ software version 1.30 (NIH). The intensity of PCNA and p27 secondary antibody staining was quantified from the average intensity of 200  $\mu\text{m}^2$  spots within individual cells. Five spots within each cell were measured and averaged. The population averaged fluorescence intensity was then determined by averaging the intensities from a population of cells at the same distance from the wall, and hence in defined extracellular environments. The error bars reflect general experimental variability due to, for example, sample to sample variability or slight photobleaching. A population of cells was defined as cells that attached within a 190  $\mu\text{m}$  region at a defined distance from the wall. The location of the cells within each population was determined with ImageJ software.

The results of PCNA and p27 staining are represented graphically as the mean  $\pm$  standard deviation from at least three similar experiments. The student's *t*-test for two samples, assuming unequal variances, was used to compare the fluorescence intensity of p27 and PCNA along the gradients. We used the data analysis package from Microsoft Excel (Microsoft Corp., Seattle, WA). A *P* value of 0.05 was considered statistically significant.

## Results

**Protein Surface Densities.** In this work we covalently immobilized both laminin and collagen I on carboxy-terminated SAMs via EDC/NHS linking chemistry.<sup>18</sup> Surface plasmon resonance measurements confirmed the irreversible protein attachment to these EDC/NHS activated monolayers (Figure 2). The difference between the initial and final water baselines gave the optical film thickness  $\Delta d$  of the protein adlayer. The protein surface densities calculated with eq 1 are given in Table 1, as are the corresponding mean fluorescence intensities measured from identical protein films. As shown in Table 1, lowering the solution concentration of laminin from 0.025 to 0.01 mg/mL decreased the MFI due to immobilized laminin by ~40%.

The surface densities of laminin on substrates modified with mixed solutions of laminin and collagen I were determined using the calibration data in Table 1. Figure 2B gives the protein densities on uniform micropatterned stripes of laminin/collagen I films prepared with laminin molar percentages of 0%, 20%, 40%, 60%, 80%, and 100%.

**Covalently Immobilized Counter Gradients of Laminin and Collagen I.** The initial protein concentrations and flow rate affected the profiles of the immobilized gradients in the main channel (Figure 3A–E). We controlled the gradient profile by decreasing the flow rate from 0.9 to 0.3  $\mu\text{L}/\text{min}$ . The initial protein solution concentrations were also varied from 7.5 to 2.5  $\mu\text{g}/\text{mL}$ . Increasing the concentration of both proteins smoothed the gradient profile and increased the gradient steepness (Figure 3A–C). In contrast, increasing the flow rate changed the profile from a continuous gradient to a stepwise gradient (Figure 3C–E).

Initially, we initiated the surface patterning by injecting one protein solution at one inlet and a buffer solution at the other inlet. This approach, however, did not generate a surface gradient (data not shown). Injecting a single protein solution simply results in a saturated substrate since the immobilization reaction is irreversible and fast. Furthermore, the amount of covalently attached protein is only limited by the surface concentration of carboxyl groups, so that even dilute protein solutions will saturate the surface over time. SPR experiments (Figure 2A) indeed showed that the SAM surfaces were saturated with laminin within 1 h of injecting an 0.1 mg/mL solution. These studies therefore established conditions required

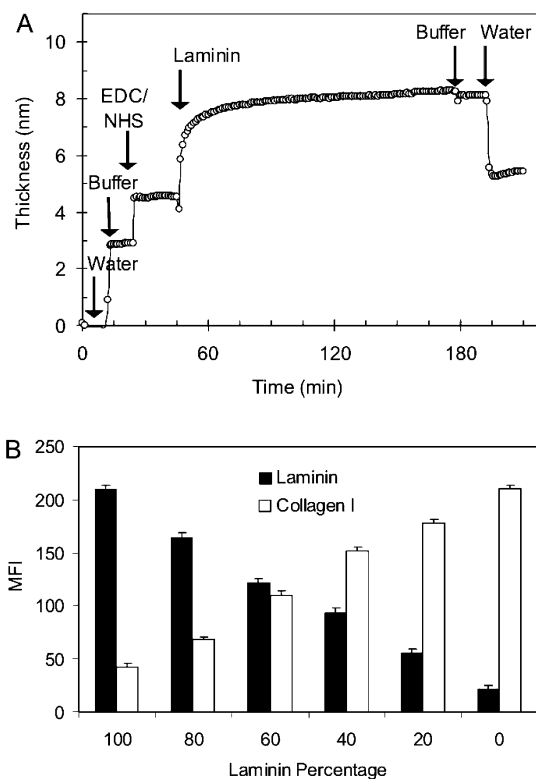


**Figure 2.** Quantification of immobilized protein surface densities. (A) The time course of the covalent functionalization of a COOH-functionalized SAM on gold was monitored by SPR. After initial flushing with water, buffer was introduced, followed by the EDC/NHS solution. Upon rinsing with buffer, the laminin injection was followed by an abrupt rise in the signal. After rinsing with buffer and then water, the difference between the two water baselines gives the effective optical thickness of the immobilized protein film. (B) The mean fluorescence intensity (MFI) of stained uniform protein stripes of laminin and collagen I prepared with laminin percentages of 0%, 20%, 40%, 60%, 80%, and 100% in the bulk solution. The corresponding protein surface densities are determined from the measured MFI and the calibration data in Table 1.

**Table 1. Mean Fluorescence Intensities (MFIs) and Surface Density of Uniform Laminin and Collagen I Films**

solution concn (mg/mL)	laminin		collagen I	
	MFI	density (pg/dm <sup>2</sup> )	MFI	density (pg/dm <sup>2</sup> )
0.025	220 $\pm$ 5	30300 $\pm$ 909	205 $\pm$ 3	36000 $\pm$ 980
0.01	160 $\pm$ 5	17090 $\pm$ 513	140 $\pm$ 5	18000 $\pm$ 550
0.005	100 $\pm$ 4	9130 $\pm$ 270	117 $\pm$ 7	12200 $\pm$ 350

to generate smooth, immobilized protein gradients with the microfluidic gradient maker in Figure 1B.

**ECM Control of Protein Expression.** The effects of relative laminin and collagen I ratios on PCNA and p27 expression were studied for cells cultured on uniform laminin and collagen I films. Prior studies demonstrated that both rat intestinal crypt-like IEC-6 cells and Caco-2<sub>BBE</sub> cells differentiate or proliferate when grown on laminin or collagen I, respectively.<sup>24,25</sup> On these uniform, mixed protein films, the cell cycle progression of IEC-6 cells, as demonstrated by PCNA expression, increased with an increasing ratio of collagen I to laminin (Figure 4A; *P* < 0.05). The p27 expression level, which correlates

(24) Basson, M. D.; Turowski, G.; Emenaker, N. J. *Exp. Cell. Res.* **1996**, *225*, 301–305.

(25) Wolpert, S. I.; Lally, K. M.; Li, J.; Wang, J.-Y.; Bass, B. L. *J. Gastrointest. Surg.* **1999**, *3*, 319–324.

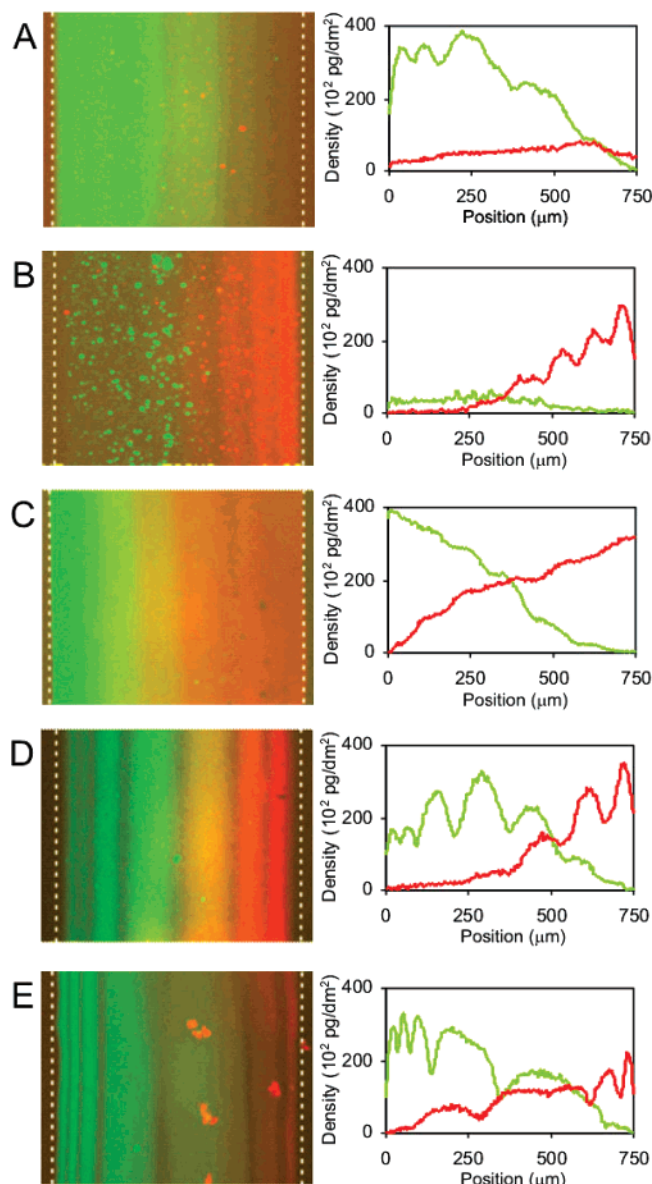


**Figure 3.** Fluorescence micrographs of surface gradients of laminin and collagen I. The quality of the gradients was optimized empirically by (i) varying initial concentrations [(A)  $C_L = 0.0075$  mg/mL,  $C_C = 0.025$  mg/mL; (B)  $C_L = 0.025$  mg/mL,  $C_C = 0.0075$  mg/mL; (C)  $C_L = 0.025$  mg/mL,  $C_C = 0.025$  mg/mL] and (ii) varying flow rates [(C) 0.0003 mL/min, (D) 0.0006 mL/min, (E) 0.0009 mL/min]. Right panels indicate the corresponding surface densities of laminin (green line) and collagen I (red line).

with cell cycle exit, increased with increasing ratios of laminin to collagen I ( $P < 0.05$ ). In comparison, the expression of PCNA in Caco-2<sub>BBE</sub> cells (Figure 4B,  $P < 0.05$ ) and CHO cells (Figure 4C,  $P < 0.05$ ) increased with increasing collagen I/laminin ratios.

The cell behavior on gradients was then quantified on the basis of the measured protein expression levels of cells at different positions on the 750-micron-wide gradient pattern. In this work, IEC-6, Caco-2<sub>BBE</sub>, and CHO cells cultured on the laminin/collagen I gradients exhibited distinct levels of gene expression related to cell cycle progression or exit. These were tracked with the local concentrations of ECM proteins at different positions of the gradient (Figures 6–8). Immunofluorescent staining of IEC-6 cells demonstrated that cells adhering to the highest laminin concentration of 27500 pg/dm<sup>2</sup> exhibited the highest p27 expression levels. The p27 expression

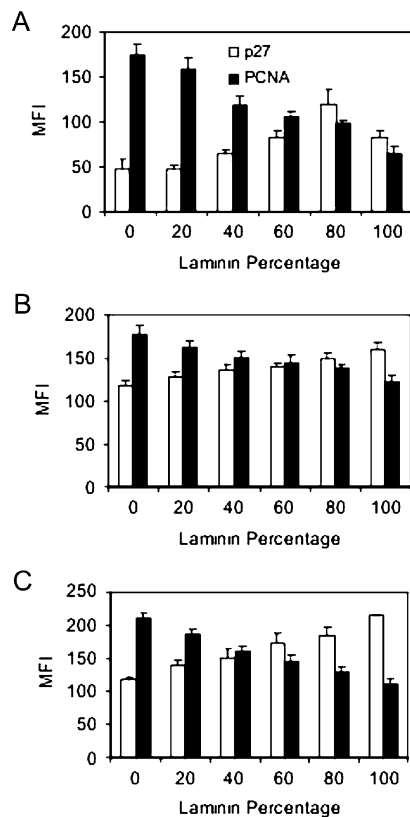


**Figure 4.** Expression of p27 and PCNA in cells cultured on uniform films of laminin and collagen I. Patterns of uniform protein composition were prepared with solutions containing different molar ratios of laminin and collagen I. The molar percentage of laminin in the bulk solution used to prepare the substrates was 0%, 20%, 40%, 60%, 80%, and 100%. After 1 day, the expression levels of p27 and PCNA were quantified by immunofluorescence in (A) IEC-6, (B) Caco-2, and (C) CHO cells.

dropped in proportion to the local laminin concentration (Figure 6,  $P < 0.05$ ). Conversely, PCNA expression was greatest in cells located at the lowest laminin concentration of 7500 pg/dm<sup>2</sup> (highest collagen I concentration). Decreasing expression levels correlated directly with the decrease in collagen I levels in the gradient (Figure 6). These results demonstrate the direct control of the cell cycle by the precise composition of an engineered ECM microenvironment.

Similar measurements were performed with Caco-2<sub>BBE</sub> and CHO cells (Figures 7 and 8;  $P < 0.05$  for each) on identical counter gradients. With both cell types, the level of p27 expression paralleled increasing laminin concentrations, and PCNA expression increased with increasing collagen I concentrations. These observations similarly demonstrate the control of cell cycle kinetics with the microfabricated ECM profiles.

The individual effects of laminin and collagen I on the cell cycle progression were studied with IEC-6 cells cultured on uniformly coated substrates of mixed films of laminin/BSA or collagen I/BSA (Figure 5). BSA was used as the second “inert” component and is presumed to have no effect on the protein expression levels. The inclusion of this background protein is necessary to block the nonspecific adsorption of other proteins in the medium. In this case, the p27 expression increased with increasing laminin (Figure 5A,  $P < 0.05$ ), but it was relatively insensitive to the collagen density (Figure 5B,  $P < 0.05$ ). On the other hand, the PCNA expression increased with increasing collagen I (Figure 5B) and also with increasing



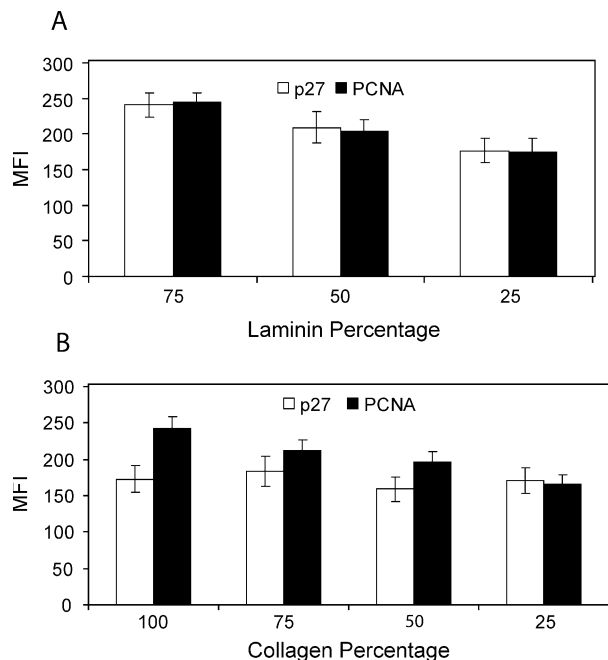


**Figure 5.** p27 and PCNA expression by IEC-6 cells cultured on uniform, laminin/BSA, and collagen I/BSA substrates. Micropatterned stripes of uniform protein composition were prepared with different percentages of (A) collagen I and (B) laminin in mixed solutions with BSA. The percentage reflects the molar percentage of the ECM protein in the protein solution used to prepare the substrate. The expression levels of p27 and PCNA in IEC-6 cells were determined after 24 h in culture.

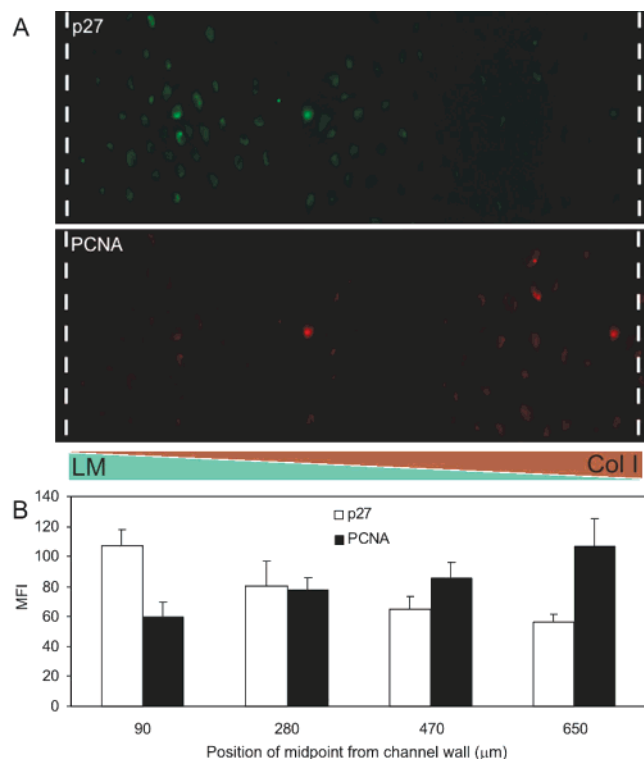


**Figure 6.** Expression of p27 and PCNA in IEC-6 cells after culturing for 1 day on 750  $\mu\text{m}$  wide gradients of laminin and collagen I. (A) The expression levels of p27 and PCNA were visualized by immunofluorescence. The wedges depict the surface concentrations of laminin and collagen I. (B) The expression levels of p27 and PCNA in IEC-6 cells were quantified from the measured MFI along the gradients.

laminin (Figure 5A). These results differ from that seen on the mixed laminin/collagen I substrates and suggest

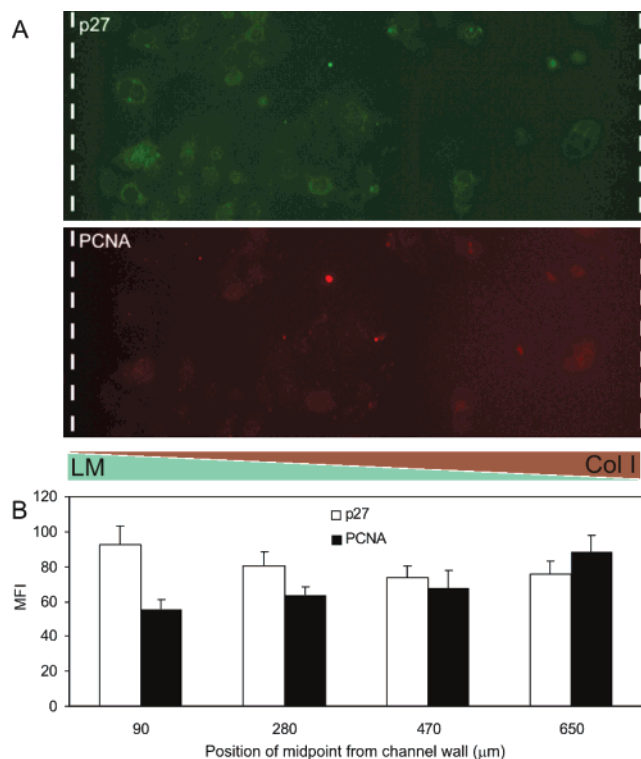


**Figure 7.** Expression of p27 and PCNA in Caco-2<sub>BBE</sub> cells cultured on 750  $\mu\text{m}$  gradients of laminin and collagen I. (A) The levels of p27 and PCNA were visualized by immunofluorescence. The wedges depict the surface concentration of laminin and collagen I. (B) The measured MFIs due to p27 and PCNA expression in Caco-2<sub>BBE</sub> were quantified along the gradients.

that the p27 and PCNA expression levels reflect the combined effect of both proteins.

Prior investigations using the gradient generator in Figure 1B showed that soluble gradients of single proteins can be immobilized on solid surfaces by physisorption.<sup>16</sup> Similar “control” studies, which are illustrated in Figure 9, show that the physisorbed gradients (Figure 9A) are not stable over time. Physisorbed counter gradients of laminin and collagen become diffuse within 24 h, when stored in culture medium in the absence of cells (Figure 9B). In contrast, the chemisorbed gradients were stable, even in the presence of cells, after 3 days (Figure 9C).

## Discussion

Using microfluidic tools, we successfully generated immobilized counter gradients of two physiologically relevant ECM proteins, laminin and collagen I, that individually promote either cell cycle exit or progression.<sup>24,25</sup> Covalent immobilization ensured ECM stability, and hence the preservation of the local ECM composition over the course of the study. The generation of gradient profiles allowed us to locally control the ECM concentration, which permitted the direct control of the cell cycle kinetics.

The quality of the gradients formed clearly depends on parameters that affect mass transport within the channels: namely, the solute concentrations and the solution flow rates. In this work, the characteristics of the gradient profiles were achieved empirically, resulting in relatively uniform increases in protein concentrations across the width of the channels.

With all three of the cell lines, p27 expression correlated directly with the local laminin concentration in the gradient. Increasing the local concentration of laminin in

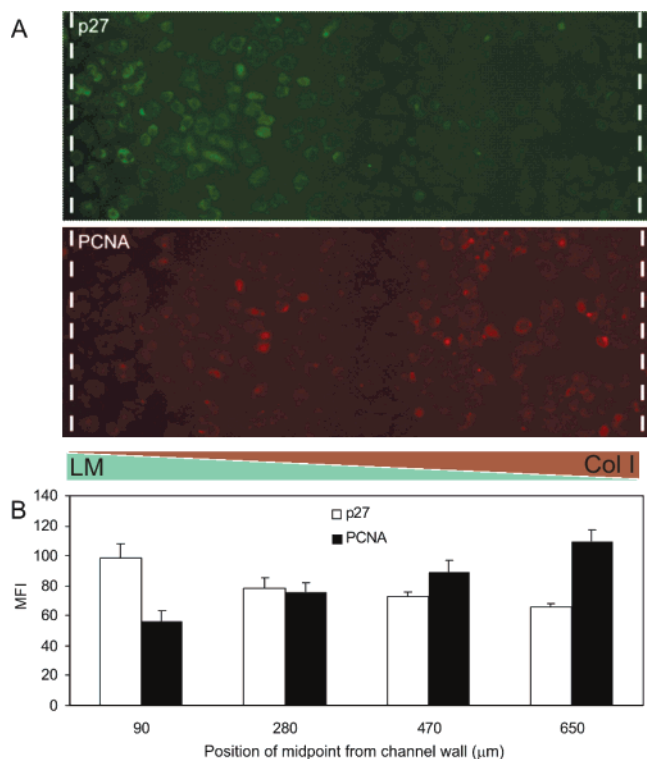


**Figure 8.** Expression of p27 and PCNA markers of CHO cells cultured on 750-micron-wide gradients of laminin and collagen I. (A) p27 and PCNA expression was visualized by immunofluorescence. The wedges depict the concentration gradients of laminin and collagen I. (B) The MFIs associated with p27 and PCNA expression by CHO cells were quantified along the gradients.

the gradient increased the expression of p27 markers. Similarly, with all three of the cell lines, PCNA expression correlated directly with the local collagen I concentration in the gradient. Thus, by culturing IEC-6, Caco-2<sub>BBE</sub>, and CHO cells on the covalently immobilized gradients, we achieved the control of cell cycle progression through the local ECM composition generated with these devices.

The individual effects of laminin and collagen I in a BSA background differed from these seen with cells cultured on the gradients. These findings confirm that the expression profiles of IEC-6 cells cultured on the laminin/collagen I gradients are determined by the relative, local amounts and identities of the two proteins on the surface.

It is important to point out that the cell behavior reported in this investigation reflects the local concentration on the gradient rather than the protein concentration difference across the cell diameter. In particular, with regard to the expression markers used in this work, the protein gradient does not appear to influence the global cell behavior. Nevertheless, the platform presented in this work enabled the rapid assessment of cell responses to multiple laminin/collagen I ratios within a single channel. Obtaining the same information with multiple, parallel protein stripes of uniform concentrations (see Figure 3B) required more fabrication steps, reagents, and time. For example, at least 20 separate protein “stripes” were used to generate the data in Figure 2B. Thus, the efficiencies inherent in this system provide additional advantages in the use of such tools for cell studies.

Alternately, the gradients themselves, rather than the average local ECM composition, may direct other cell behavior such as migration or axon extension. While this was not the focus of the studies presented here, cell

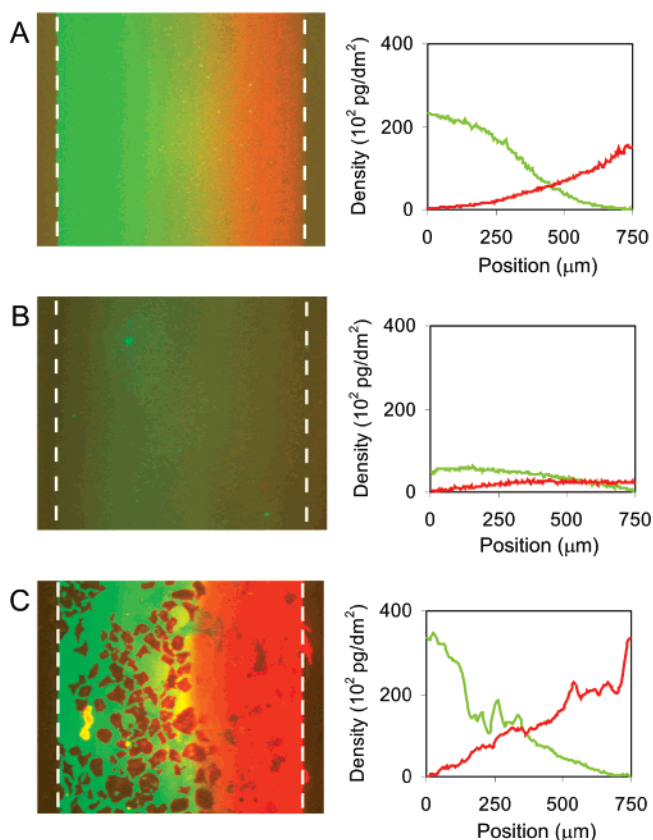


**Figure 9.** Fluorescence images of laminin and collagen I gradients (left-hand column) and the corresponding protein density profiles (right-hand column). (A) Physically adsorbed gradients of laminin and collagen I were visualized by immunofluorescence immediately after the gradients were prepared. (B) Profile of the physically adsorbed gradient after 1 day in culture medium at 37 °C. (C) Profile of a covalently bound gradient measured after IEC-6 cells were cultured on the gradients for 3 days.

behavior distinctly driven by the protein concentration profile is the subject of future work.<sup>16</sup> This investigation defined the design rules, which determine the characteristics of covalently immobilized protein gradients, and further demonstrated the control of gene expression through the precise control of the local ECM composition.

We attribute the regiospecific cell behavior over the course of the study to the influence of the ECM profile generated with the gradient tool, because of the stability of the covalently bound protein gradients. Immunofluorescence staining of the protein gradients before and after cell culture demonstrated the stability of ECM patterns for up to 3 days in the presence or absence of cells. This indicates that the immobilized protein gradients did not degrade and that the cells did not significantly remodel the ECM during the assays. By contrast, in control experiments physisorbed protein gradients maintained in media became diffuse when kept in media for 1 day (Figure 9B). We also carried out all of our cell culture experiments in serum-free medium, to prevent changes in the ECM composition through the nonspecific adsorption of serum proteins. We were thus able to manipulate cell behavior directly through precise control of the local protein concentration as defined by their spatial position on the protein gradient.

## Conclusions

This work demonstrates the fabrication of stable, covalently immobilized gradients of different ECM pro-

teins, and the spatial variation of cellular responses directed by these engineered ECM patterns in vitro. IEC-6, Caco-2, and CHO cells exhibited regiospecific expression of p27 and PCNA, markers that are linked to the cell cycle progression, when cultured on immobilized counter gradients of the ECM proteins laminin and collagen I. This prototype system thus represents a powerful and versatile methodology for creating in vitro models of ECM environments for uniquely and quantitatively testing such hypotheses. It is simple and broadly portable to various cell types and other ECM proteins and overcomes the major problem of gradual gradient remodeling that has limited the use of physisorbed gradients to short-term biological studies.

These platforms with covalently immobilized gradients promise to engender a wide range of previously difficult, quantitative investigations of cell growth and differentiation in response to different protein combinations in a variety of concentration profiles. These microfluidic tools will thus enable new investigations of fundamental cell biology, as well as contribute to the establishment of quantitative biological design rules for controlling cell growth, migration, differentiation, and function.

**Acknowledgment.** This work was supported by a Critical Research Initiative grant from the Campus Research Board at UIUC.

LA048303K